International Journal of
Research in Chemistry and Environment
Available online at: www.ijrce.org
ISSN 2248-9649

Research Paper

Ab initio investigation on the IOOBr isomers and reaction pathways of the IO+BrO reaction

***T. K. Ghosh[1] and S. Yabushita[2]**
[1]Department of Physics, Diamond Harbour Women's University, Sarisha
DH Road, South 24-Pgs, West Bengal-743368, INDIA
[2]Department of Chemistry, Faculty of Science and Technology, Keio University,
3-14-1 Hiyoshi, Kohoku-ku, Yokohama, 223-8522, JAPAN

(Received 26th July 2019, Accepted 04th October 2019)

Abstract: *Various minimum energy geometries, transition state geometries and possible reaction pathways have been investigated at the ab initio level of theories for the atmospheric important reaction between IO and BrO radicals. We employed SDB (Stuttgert-Dresden-Bonn)-cc-pVTZ basis sets for bromine and iodine and cc-pVTZ basis set for oxygen augmented with a set of diffuse functions (s,p) for each atom. The geometries and energetics have been studied at the MP2 and QCISD(T)//MP2 levels of theory, respectively. Possible reaction pathways for different product channels have been discussed on the basis of structural information and energetics along with results of the IRC calculations.*

Keywords: *Ab initio* investigation, Ozone depleting systems, Equilibrium geometries, Transition state geometries, Energetics, Reaction pathways, IOOBr isomers.

Introduction

The halogen monoxide radicals play a significant role in the catalytic depletion of ozone layer. Chemistry involving iodine is of particular importance, since its minimal contribution can make a significant impact upon atmospheric ozone depletion[1-3]. The role of iodine in atmospheric ozone depletion depends upon several factors and one depends on kinetic data of the key reactions of IO with ClO, BrO and HO_2, which are also called the rate-limiting steps in catalytic cycles[1]. The reaction IO + BrO is thus one of the key reactions potentially important for such atmospheric ozone depletion processes, especially in the lower stratosphere. As the stratospheric abundance of BrO radicals is generally greater than IO radicals, this reaction may occur significantly even at low IO concentrations. In addition, this reaction has also a potential contribution in tropospheric chemistry, particularly in the marine boundary layer and in the Arctic lower troposphere, where ozone depletion events observed in recent years[4-7].

Solomon et al. are the first who raised the role of iodine in stratospheric chemistry based on a model calculation[1]. Considering only the products I + X + O_2 for IO + XO (X = Cl, Br) reactions and assuming both reactions proceed with rate constants of $1x10^{-10}$ $cm^3molecule^{-1}s^{-1}$, they predicted that iodine is 1000 times more efficient than chlorine in destroying ozone in the lower stratosphere. Later, Bedjanian et al.[8,9], Gilles et al.[10] and also Turnipseed et al.[11,12] claimed from their experimental investigations on IO + XO (X = Cl, Br) that iodine is about 3-5 times less efficient than model prediction of Solomon at al.[1] This relative efficiency could even be lowered if the IO + BrO reaction does not lead to 100% net production of I + Br + O_2, as was assumed by Solomon et al.[1].

The reaction between IO and BrO radicals may proceed through the following channels:

IO + BrO → Br + OIO (1)
→ I +BrOO → I + Br + O_2 (2)
→ IBr + $^3O_2$ (3)
→ I + OBrO (4)

Bedjanian et al.[9] performed an extensive study on this IO + BrO reaction using discharge flow mass spectrometric technique and predicted an overall rate constant of $(8.5\pm1.5)x10^{-11}$ $cm^3molecule^{-1}s^{-1}$ at room temperature in comparison to the model value of $1.0x10^{-10}$ $cm^3molecule^{-1}s^{-1}$. According to Bedjanian et al.[9], the major channel is (1) forming Br + OIO and has a branching ratio of 0.65-1.0. Since XOO (X = Br, or I) dissociates to X + O_2, the channel (2) is responsible for forming I+Br+O_2 products. The channels (2) and (4) were studied to have branching rations < 0.2 and < 0.3, respectively[9]. The third channel (3) is considered the minor one, leading to a branching ratio of < 0.05[9]. At a subsequent time, Gilles et al.[10] investigated this IO + BrO reaction using pulsed laser photolysis with discharge flow technique and predicted that the non-iodine atom producing channels 1 and 3 are the dominant ones. Rowley et al.[13] using a technique of laser flash photolysis with UV absorption spectroscopy examined the IO+BrO reaction and predicted a value of $(8.5\pm1.4)x10^{-11}$ $cm^3molecule^{-1}s^{-1}$ at 298K. Rowley et al.[13] mentioned that the potential impact of channel (1) and (3) on ozone depletion depends on the fate of OXO species, whether they are photostable or not. According to experimental investigations[9,10], channel(1) is slightly exothermic, channel (2) is also exothermic to form I+Br+O_2, channel (3) is highly exothermic, but channel (4) is endothermic. This thermal kinetics is also supported by our recent report, discussed later.

Although, several experimental investigations have been performed for determining the rate constant and branching ratios of this radical-radical reaction[9,10,12,13], there is a complete lack of information on the intermediate states, energy barriers and as well as on the reaction pathways for the different product formations of this atmospheric important reaction. Regarding the reaction pathways, only Johnsson et al.[14] from a photoisomerization study of related ClOOI isomer using the R-matrix isolation technique suggested that a Y-shaped compound has been converted to the thermodynamically favored products ICl and O_2. Among the theoretical calculations along this line, Francisco group[15], Melissas et al.[16] and Gomez and Pacios[17] carried out *ab initio* calculations of the different isomers of XOOY (X, Y = I, Br and Cl atoms) and studied their geometries, frequencies and energetics. Melissas et al.[16] have reported structure and frequency of IOOX isomers at the MP2/ECPnMWB level of theory. Papayannis et al. performed *ab initio* calculations on the BrO self-reaction and BrO+ClO reaction[18,19] and suggested several reaction pathways. Previously, we reported spectroscopic constants and thermochemical properties of various reactants and products involved in the reactions IO with ClO and BrO and also the heat of reaction of various channels using an extensive basis set at the QCISD//MP2 level of theory[20]. In a recent article, we have reported structural information of the isomers IOOCl and the possible reaction pathways of the IO+ClO reaction[21].

In the present article, we shall report various minimum energy geometries and transition state geometries, which are possibly involved in the course of this atmospheric important IO+BrO reaction. Possible reaction pathways for the different product channels of this reaction have been discussed. To the best of our knowledge, this is the first theoretical investigation on the IO + BrO reaction pathways and about all the isomeric configurations involved in the reaction pathways. We explain the computational schemes involved, followed by results and discussion of the present investigation in the following sections.

Computational Details

We primarily employed a large-core pseudopotential and correlation-consistent SDB (Stuttgert-Dresden-Bonn)-cc-pVTZ basis sets for bromine and iodine[22] and cc-pVTZ basis set for oxygen atom[23]. Basically, it is a frozen-core electron method as the core electrons have been substituted by effective core potentials. All atoms basis sets were then augmented by a set of (s,p) diffuse functions[22,23]. All the minimum energy geometries and transition state geometries were optimized at the MP2 level of theory. Vibrational frequencies were calculated at the MP2 level of theory, too. Energetics of all the species were studied at the QCISD(T)//MP2 level. In calculating relative energies of the different species with respect to the reactants (IO+BrO), we included zero-point energy (ZPE) corrections of different species obtained using our MP2 frequency values without using any scaling factor, and experimental spin-orbit coupling (ΔSOC) corrections of Br (3.51 kcal mol^{-1})[24], I (7.25 kcal mol^{-1})[24], BrO (1.38 kcal mol^{-1})[25] and IO (93.33 kcal mol^{-1})[26].

The intrinsic reaction coordinate (IRC) method was used to retrieve the minimum energy paths on both sides for all the transition states. We used MP2 method for the IRC calculations with different step sizes for different cases ranging between 0.1-0.01 $amu^{1/2}$bohr. Results of the IRC calculations help us to analyze possible reaction pathways for different product channels. We have used Gaussian W03 suite of programs for all the calculations described above[27].

Results and Discussion

A: Minimum energy geometries

The geometry and vibrational frequencies of various minimum energy geometries and transition state geometries involved in the reaction IO+BrO have been identified at the MP2 level of theory.

Table 1: Optimized Minimum Energy Geometries (A^o, degree), Harmonic Frequencies (cm^{-1}) of IOOBr isomers at the MP2 level

Species	Geometry			Frequency		
	Coordinate	Present Calc.	Others Calc.[b]	Mode Description	Present Calc.	Others Calc.[b]
MG(a) OIOBr	OI	2.0294	2.055	IO´ str	944.9	934
	IO´[a]	1.8050	1.819	O´Br str	628.3	630
	O´Br	1.8465	1.852	OI str	442.8	438
	IO´Br	114.1	113.6	OIO´ bnd	222.7	215
	OIO´	107.6	108.6	IO´Br bnd	147.9	141
	OIO´Br	74.6	71.2	Torsion	65.5	62
MG(b) BrOOI	BrO´	1.8571	1.870	O´O str	754.5	761
	O´O	1.4142	1.403	BrO´ str	601.3	597
	OI	2.0378	2.064	OI str	546.4	536
	BrO´O	109.8	110.1	BrO´O bend	355.9	350
	O´OI	110.6	110.9	O´OI bend	242.1	239
	BrOOI	84.6	83.0	Torsion	70.0	72
MG(c) $IBrO_2$	IBr	2.7464	2.725	BrO str asym	1077.1	1058
	BrO	1.5974	1.603	BrO str sym	1057.5	1036
	IBrO	104.7	104.7	OBrO bend	382.1	380
	OBrO	112.0	112.2	IBr str	267.1	272
	IBrOO	-112.8		IBrO bend	155.6	156
				Umbrella	134.4	144
MG(d) $BrIO_2$	BrI	2.5694	2.568	IO str asym	976.6	959
	IO	1.7732	1.786	IO str sym	973.0	953
	BrIO	102.6	102.6	BrI str	249.8	253
	OIO	109.0	111.0	OIO bend	308.1	303
	BrIOO	-108.3		Umbrella	176.4	181
				BrIO bend	154.2	153
MG(e) IOBrO	IO	2.0185	2.037	BrO´ str	1034.0	1022
	OBr	1.8861	1.894	IO str	568.9	573
	BrO´	1.6305	1.636	OBr str	416.8	417
	IOBr	113.3	113.3	OBrO´	260.5	258
	OBrO´	111.4	111.8	IOBr bend	145.8	141
	IOBrO´	66.4	63.3	Torsion	57.7	52

Abbreviations: [a] O´ is the O-atom attached to Br-atom, [b]Reference[16].

In Table 1, we have listed our results of various optimized minimum energy geometries and the vibrational frequencies.

The first isomer, OIOBr denoted as MG(a) herein, is a linear chain-typed structure with bromine as terminal atom and has a OIO´Br dihedral angle of 74.6^o (O´ is the O-atom attached to Br-atom). The IO´Br bond angle (114.1^o) is larger than the OIO´ bond angle (107.6^o). The Mulliken atomic charges on OIO´Br are -0.49 for O, 0.97 for I and –0.64 for O´ and 0.16 for Br, respectively, and suggest the presence of X^+O^- (X=Br,I) resonant structures. An natural bond order analysis may reveal interesting behavoiur about the species. The O-O´ distance (3.098 Å) being smaller than the I-Br one (3.254 Å), not shown in the table, makes O-O´ repulsion larger than the Br-I one. But the dominant OI and IO´ resonances decrease the net O-O´ repulsion compared to I-Br one and thereby IO´Br angle becomes larger than the OIO´ one.

The second isomer, BrOOI denoted as MG(b) herein, is the skewed BrOOI denoting a dihedral angle of 84.6^o. The O´OI bond angle (110.6 ^{o}) is almost close to the BrO´O one (109.8^o). The Br-O´ and O-I distances are larger than the O´-O distance by 6 Å, which may follow due to the better overlap of the 4p orbital of bromine and the 5p orbital of iodine with the 2p orbital

of oxygen than the similar 2p orbitals in oxygen atoms. An NBO analysis may reveal the true picture about this isomer.

Third and fourth isomers are the Y-shaped $IBrO_2$ and $BrIO_2$, denoted as MG(c) and MG(d), respectively, both of them exhibiting a plane of symmetry (C_S symmetry). In case of $IBrO_2$, the Br-O bond length (1.5974 Å) is much smaller than the I-Br bond length (2.7464 Å) due to the multiple bonding characteristic of Br=O. The OBrO angle is formed by the repulsion of lone pair electrons of bromine, the two oxygen atoms and the Br=O bonding electrons. The IBrO angle is formed by the repulsion of lone pairs of terminal oxygen atoms, Br=O bonds and the I-Br bond. The former repulsion being greater than the latter one makes the OBrO angle (112.0°) larger than the IBrO angle (104.7°). A similar explanation holds for the second Y-shaped geometry of MG(d) $BrIO_2$. The central iodine atom being larger than the bromine makes the I=O bond larger (1.7732 Å) in MG(d) $BrIO_2$ than the Br=O bond (1.5974 Å) in MG(c) $IBrO_2$. The Br-I bond length in $BrIO_2$ is found to be smaller than the I-Br bond length in $IBrO_2$.

The fifth one IOBrO, denoted as MG(e) herein, exhibits a linear chain-type structure and has a dihedral angle IOBrO´ of 66.4°. Like the MG(a) OIOBr isomer, it also adopts X^+O^- (X=I, Br) resonant structures and the Mulliken charges on the atoms are 0.29 for I, -0.49 for O, 0.78 for Br and –0.58 for O´, respectively. Although, the O-O´ repulsion is larger than the I-Br one, the dominant O-Br and Br-O´ resonances decrease the net O-O´ repulsion, which in turn makes the OBrO´ angle slightly smaller than the IOBr angle. The available theoretical data by Melissas et al.[16] at the MP2/ECPnMWB level of theory are tabulated for comparison and it shows that our calculated geometry are very much consistent with their reported values.

The frequency values of the minimum energy geometries are listed in Table 1. We see that the MG(a) OIOBr isomer has I-O´ and O-I stretching frequencies of 944.9 cm^{-1} and 442.8 cm^{-1}, respectively. The OIO´ bending has a larger frequency than the IO´Br bending and it is consistent with the smaller OIO´ angle than the IO´Br one. The MG(b) BrOOI isomer has the largest frequency of 754.5 cm^{-1} associated with the O´-O stretching mode and the least one of 70.0 cm^{-1} associated with a BrOOI torsion mode. The Br-O´ stretch has a larger frequency (601.3 cm^{-1}) than the O-I stretch (546.4 cm^{-1}) and is consistent with Br-O' bond length being smaller than the O-I one. Further, the O´OI bend has a smaller frequency than the BrO´O one due to the larger mass of iodine than that of bromine. The third isomer MG(c) $IBrO_2$ has Br-O symmetric and asymmetric stretching frequencies of 1077.1 cm^{-1} and 1057.5 cm^{-1}, respectively. The I-Br symmetric stretching occurs at the value of 267.1 cm^{-1}, which is very small compared to the Br-O stretching frequency and it is consistent with the I-Br bond length being larger than the Br-O one. There is an umbrella mode having a frequency of 133.4 cm^{-1}. The MG(d) $BrIO_2$ isomer has also larger frequency values associated with I-O symmetric and asymmetric stretching modes. The Br-I stretching frequency is smaller than the I-O one due to the similar reason of larger Br-I bond length than the I-O one. It also has a similar umbrella mode with a frequency of 176.4 cm^{-1}. The fifth isomer MG(e) IOBrO' has a maximum frequency of 1034.0 cm^{-1} associated with the Br-O´ stretch. The OBrO´ and IOBr bends occur at 260.5 cm^{-1} and 145.8 cm^{-1}, respectively, which are consistent with the respective bond angle values. The least one is the IOBrO´ torsion adopts a frequency of 57.7 cm^{-1}. The available frequency values by Melissas et al.[16] at the MP2/ECPnMWB level of theory are also tabulated for comparison and it shows that our calculated frequency values are also consistent with them, except the stretching frequency for $IBrO_2$ and $BrIO_2$ are differ by about 10-20 cm^{-1} only.

B: Transition state geometries

The geometries of various transition states are depicted in Table 2. The first one is TS(a) BrOIO and has a linear chain-typed structure with BrO´IO dihedral angle of 84.2° (where O´ is the O-atom attached to the Br). The Br-O´ bond length is larger than both O´-I and I-O bonds and it is probably due to the smaller orbital overlap between Br and O´ than that between O´ or O and I. The second one TS(b) IOOBr also has a chain structure with an IOO´Br dihedral angle equal to 56.4°. The IOO´ bond angle (108.8 °) is larger than the OO'Br one (99.2°) due to the larger repulsion of iodide with oxygen atoms than that between bromine and oxygen atoms. The third one TS(c) BrIOO exhibits large Br-I and O-O´ bonds. The IO and IO´ bond distances are not equal as in the case of Y-shaped $BrIO_2$ isomer. The fourth transition state reported here is a cis-form of the TS(d) cis-BrOOI intermediate. The BrO´O angle is smaller than the O´OI one due to the smaller repulsion effect associated with the smaller size of the bromine atom compared to larger one of the iodine atom. We have also examined the trans- form of BrOOI intermediate, but it could not be recognized as a transition state at the present MP2 level of theory. We have also identified two more transitions states (IOBrO and IBrOO), but they have very large barrier heights of more than 11.4 kcal mol^{-1} at the QCISD(T) level. These are out of our present interests and due to this reason we did not report them here.

The harmonic frequencies of all the transition states are also listed in Table 2. Note that, all four transition states are characterized by one imaginary frequency, suggesting that these are first-order saddle points. The first one, the TS(a) BrOIO has larger frequencies

associated with IO and O´I stretches. Two bends, O´IO and BrO´I, occur at 289.7 cm^{-1} and 101.0 cm^{-1}, respectively. It has a torsional mode with a frequency of only 54.3 cm^{-1}, which may be treated as a hindered rotor model. For the transition state TS(b) IOOBr, the O-O stretching mode has a maximum frequency of 1236.9 cm^{-1}. The least one is associated with the I-Br stretch with a frequency of 91.4 cm^{-1}. The third transition state TS(c) BrIOO, has larger frequencies associated with BrO´ (1105.6 cm^{-1}) and BrO (945.6 cm^{-1}) stretches, which are consistent with the bond distances BrO (2.8277 Å) and BrO´ (4.2159 Å), and it also exhibits the O´ atom much closer to the Br one than the other O atom. The OBrO´ and BrIO bends occur at 115.6 cm^{-1} and 69.5 cm^{-1}, respectively. The fourth transition state TS(d) cis-BrOOI has larger frequencies associated with the Br-O´ stretch, the BrO´O bend and the O-I stretch. The IOO´ bending frequency is smaller than the BrO´O bending frequency due to the heavier iodine mass than the bromine one. There is no data available at the theoretical level for comparison purposes.

Table 2: Optimized Transition State Geometries (A°, degree), Harmonic Frequencies (cm^{-1}) of various transition states at the MP2 level

Species	Geometry		Frequency	
	Coordinate	Present Calc.	Mode Description	Present Calc.
TS(a) BrOIO	BrO´	2.6392	IO str	978.2
	O´I	1.8104	O´I str	736.6
	IO	1.7808	O´IO str	289.7
	BrO´I	111.5	BrO´I bend	101.0
	O´IO	111.4	Torsion	54.3
	BrO´IO	84.2	Reaction coord	206.9i
TS(b) IOOBr	IO	1.9712	OO´ str	1236.9
	OO´	1.3313	IOO´ bend	625.7
	O´Br	2.7604	IOO´ wag	373.3
	IOO´	108.8	O´Br str	279.6
	OO´Br	99.2	IBr str	91.4
	IOO´Br	56.4	Reaction coord	299.6i
TS(c) BrIOO	BrI	3.2663	BrO´ str	1105.6
	IO	1.7987	BrO str	945.6
	OO´	2.9417	OO´ str	293.5
	IO´	1.7721	BrO´I bend	115.6
	BrO	2.8277	BrO´O bend	69.5
	BrO´	4.2159	Reaction coord	695.5i
	BrO´I	87.3		
	BrO´O	93.9		
	OIO´Br	-100.7		
TS(d) cis-BrOOI	BrO´	1.8113	BrO´ str	707.6
	O´O	1.5170	BrO´O bend	600.9
	OI	1.9902	OI str	520.6
	BrO´O	117.2	OO str	343.0
	O´OI	119.5	O´OI bend	121.2
			Reaction coord	213.6i

C: Energetics and Reaction pathways

In Table 3, we list electronic energies of all isomers, transition states, reactants and products obtained at the MP2 and QCISD(T) levels of theory. The MP2 energies predict inconsistent relative energies. The listed QCISD(T) single-point energies are zero-point corrected at the MP2 level and experimental SOC corrections are also included for available species. Spin-orbit coupling (SOC) corrections have not been considered for the tri- and tetra- atomic systems in the present study. The Mulliken population analyses show that the radical side of the OIO and OBrO are on the I and Br atoms, respectively. The I atom spin density is greater than O´s one in OIO and the Br spin density is smaller than those of the O atoms in OBrO. Thus the SOC correction of OIO is not negligible and should be taken in to account to acquire better reaction energetics. For IOO or BrOO, the radical side is on the terminal O atom and the spin density of I or Br is smaller compared to the O atoms. So the SOC corrections are

less important for IOO and BrOO systems. Experimental SOC corrections are not available for tetra-atomic systems in literature.

Among the five isomeric geometries, MG(d) $BrIO_2$ is the most stable isomer and it is 27.20 kcal mol^{-1} below the reactants (IO+BrO). The other isomers, MG(b) BrOOI, MG(a) OIOBr, MG(e) IOBrO and MG(c) $IBrO_2$ are considered less stable and lie below reactants by 17.35 kcal.mol^{-1}, 15.71 kcal.mol^{-1}, 7.46 kcal.mol^{-1} and 0.48 kcal.mol^{-1}, respectively. The transition states TS(a) BrOIO, TS(c) BrIOO and TS(b) IOOBr lie above reactants by 2.23 kcal.mol^{-1}, 3.99 kcal mol^{-1} and 8.43 kcal.mol^{-1}, respectively. Only the TS(d) cis-BrOOI is at 7.21 kcal.mol^{-1} below reactants. An energetics table of equilibrium geometries wrto MG(b) BrOOI has been prepared in Table 3 along with the results of Melissas et al.[16] for comparison.

Table 3: Total Electronic Energies (a.u.), ZPE (kcal mol^{-1}) and SOC Corrections (kcal mol^{-1}) and Relative Energy (kcal mol^{-1}) of Various Species Involved in IO+BrO Reaction

Species	E_e		ZPE[b]	SOC[c]	ΔE_{corr}[d]	Relative energy wrto MG(b)	
	MP2	QCISD(T)				Our	Others[e]
Reactants[a] IO + BrO	-174.641270	-174.737025	2.05	-4.71	0.00		
Minimum energy geometries							
MG(a) OIOBr	-174.718789	-174.771891	3.51		-15.71	1.64	0.8
MG(b) BrOOI	-174.712762	-174.774768	3.67		-17.35	00.0	00.0
MG(c) $IBrO_2$	-174.695100	-174.749025	4.39		-0.48	16.87	16.1
MG(d) $BrIO_2$	-174.741008	-174.791079	4.06		-27.20	-9.85	-8.0
MG(e) IOBrO	-174.704806	-174.758810	3.55		-7.46	9.89	7.1
Transition state geometries							
TS(a) BrOIO	-174.680379	-174.742639	3.09		2.23		
TS(b) IOOBr	-174.670172	-174.733769	3.73		8.43		
TS(c) BrIOO	-174.682020	-174.740673	3.62		3.99		
TS(d) cis-BrOOI	-174.697414	-174.757984	3.28		-7.21		

Abbreviations: [a]Reference[12], [b] Calculated using our MP2 frequencies, [c]Reference[25,26], [d]Energy differences with respect to reactants (used QCISD(T) energies including ZPE and SOC corrections). [e]Reference[16].

IRC calculations performed at the MP2 level exhibit the minimum energy paths of reaction pathways for every channel and they are represented in Figures 1-5. In these Figures, energetic of different species are shown in an arbitrary vertical scale.

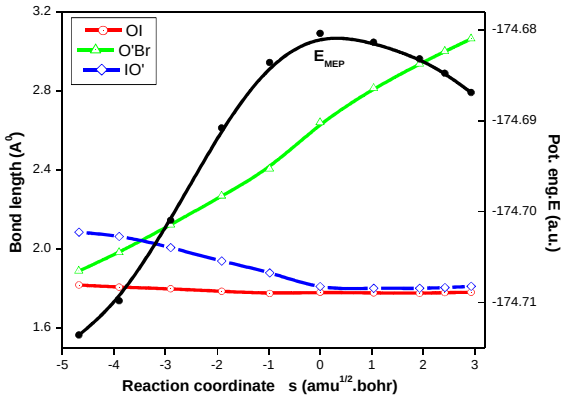

Figure 1: IRC result: MG(a) OIOBr - TS(a) BrOIO - Br+OIO

The transition state TS(a) BrOIO represents the energy barrier to the formation of Br + OIO, i.e, channel (1) in the forward direction. This is clearly depicted in Figure 1 by the results of the IRC calculation, where the Br atom approaches far from O´ with simultaneous approach of O´-I and I-O to equal value. The backward IRC calculation reaches to the isomer MG(a) OIOBr.

We found three isomeric interconversion processes via TS(b) IOOBr, TS(c) BrIOO and TS(d) cis-BrOOI. The TS(b) IOOBr represents the energy barrier for the first isomeric interconversion process from MG(b) BrOOI to MG(c) $IBrO_2$. This can be visualized by the geometrical change, in Figure 2, that where a shrinkage of the I-Br bond length from MG(b) to MG(c) via TS(b), viz., 3.700 Å to 3.331 Å and then to 2.746 Å and a corresponding increase of the I-O bond length viz. 2.861 Å to 2.712 Å and then to 3.510 Å are clearly depicted.

The second isomeric interconversition is MG(c) $IBrO_2$ to MG(d) $BrIO_2$, which occurs via TS(c) BrIOO. This can be visualized by the geometrical change, shown in Figure 3, namely, the decrease of the Br-O bond length

from MG(c) $IBrO_2$ via TS(c) BrIOO to MG(d) $BrIO_2$, viz., 2.746 Å to 2.8277 Å and then to 3.409 Å, while the I-O and I-O´ bonds approach each other. It is to be mentioned that, we could not proceed further the IRC calculation towards the negative reaction coordinate side because of convergence problems. The energy value of the last geometry obtained in IRC calculation is found to be very close to MG(c) $IBrO_2$, which is 0.00164 au only above the MG(c).

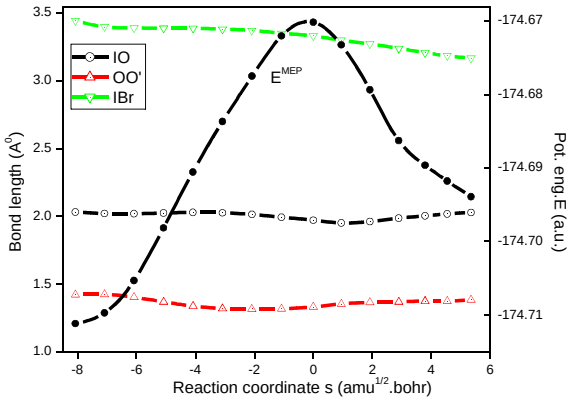

Figure 2: IRC result: MG(b) BrOOI - TS(b) IOOBr - MG(c) $IBrO_2$

Finally, the third isomeric interconversion process is MG(b) BrOOI to MG(e) IOBrO via TS(d) cis-BrOOI. This can also be clearly visualized in Figure 4 by the geometrical alterations along the MEP, namely a slight shrinkage of the Br-O´ distance from MG(b) BrO´OI to MG(e) IOBrO´ via TS(d) cis-BrOOI viz., 1.8571 Å to 1.8113 Å and then to 1.6305 Å and a simultaneous increase of O-O´ distance viz., 1.4142 Å to 1.5170 Å and then to 1.5270 Å. We could not proceed any further the IRC calculation towards the forward direction to further decrease the BrO distance.

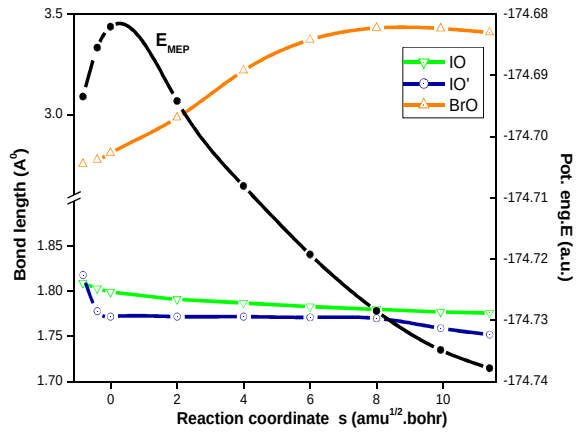

Figure 3: IRC Result MG(c) $IBrO_2$ - TS(c) BrIOO - MG(d) $BrIO_2$

All the reaction pathways, as obtained from IRC calculations, of the aforementioned reaction are shown in Figure 5 using coloured lines. The energy barrier for the first transition state TS(a) BrOIO is quite large and equal to 17.94 kcal mol^{-1} with respect to MG(a) OIOBr. So the channel (1) Br + OIO, may be depicted to be formed by the initial formation of MG(a) OIOBr isomer followed by a direct dissociation to form the Br + OIO products. It is considered a rapid process, which also supports the computation of a large rate constant. Within the second channel (2), I + BrOO may likely be described by a direct dissociation process from the MG(b) BrOOI isomer. Since MG(b) BrOOI isomer lies below the MG(a) OIOBr one, the probability of occurring channel (2) will be less than the channel (1).

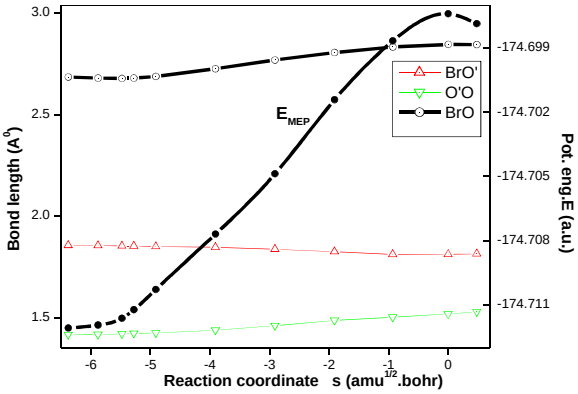

Figure 4: IRC Result MG(b) BrOOI - TS(d) cis-BrOOI - MG(d) IOBrO

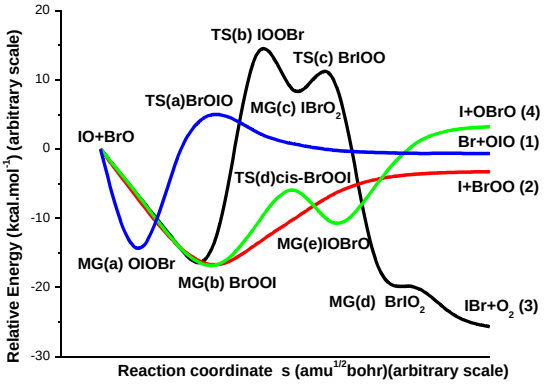

Figure 5: Reaction pathways to different channels

The energy barrier for the first isomeric interconversion process MG(b) BrOOI to MG(c) $IBrO_2$ via TS(b) IOOBr is quite large and equal to 25.78 kcal mol^{-1}, so it is unlikely possible to occur. Therefore, a direct formation of the MG(c) $IBrO_2$ isomer may lead to the second isomeric interconversion process MG(c) $IBrO_2$ to MG(d) $BrIO_2$ via TS(c) BrIOO to form the most stable isomer MG(d) $BrIO_2$. Following the suggestion of Johnsson et al.[14], as in the case of ICl + $^3O_2$ formation, one can expect the formation of channel (3), i.e., IBr + $^3O_2$, via the Y-shaped isomer MG(d) $BrIO_2$ by the spin-orbit quenching somewhere in the exit channel or by the removal of the restriction of spin

conservation due to the presence of heavy atoms. Such a possibility for the removal of spin conservation restriction promoted by heavy atoms has been mentioned earlier by Papayannis et al.[19] and others[21]. The multi-step process of forming channel (3) $IBr+O_2$, is considered a minor channel. This qualitative picture is in agreement with experimental branching ratio trends[9]. The channel (4) I + OBrO may occur via the cis-transition state TS(d) cis-BrOOI. Its larger barrier height suggests a smaller rate constant than channel's (2). Its endothermocity nature[20] also supports the occurrence of smaller rate constant.

Conclusion

In conclusion, various equilibrium and stationary structures have been investigated using *ab initio* methods for the isomers IOOBr formation, which are involved during the course of the atmospheric important ozone depleting IO + BrO reaction. Possible reaction pathways for different product formations are also discussed on the basis of IRC calculations and energetic of the isomers. Most data reported within this article are freshly new and may serve as future references. These data may be of great help in investigating atmospheric implications of such systems in ozone depletion.

Acknowledgments

One of the authors TKG gratefully acknowledges the Department of Science & Technology and Biotechnology, Govt. of West Bengal, India for a financial support under the Project No. 357(Sanc.)/ST/P/S&T/16G-26/2018. TKG also acknowledges the Japan Science and Technology Corporation (JSTS) and the Ministry of Education, Science, Culture and Sports of Japan for a part of this research work with SY at the Keio University, Japan.

References

1. Solomon S., Garcia R.R. and Ravishankara A.R., On the role of iodine in ozone depletion, *J. Geophys. Res*., **99,** 20491 (**1994**)

2. Solomon S., Burkholder J.B., Ravishankara A.R. and Garcia R.R., Ozone depletion and global warming potential of iodine, *J. Geophys. Res*., **99,** 20929 (**1994**)

3. World Meteorological Organization/United Nations Environment Programme (WMO/UNEP): Scientific assessment of ozone depletion, Geneva, WMO Rep., **25** (**1992**)

4. Anderson J.G., Toohey D.W. and Brune W.H., Free radicals within the antarctic vortex: The role of CFCs in antarctic ozone loss, *Science*, **251**, 39 (**1991**)

5. Chameides W.L. and Davis D.D., Iodine: Its possible role in tropospheric photochemistry, *J. Geophys. Res.*, **85,** 7383 **(1980)**

6. Stutz J., Hebestreit K., Alicke B. and Platt U., Chemistry of halogen oxides in the troposphere: Comparison of model and calculations with recent field data, *J. Atmos. Chem*., **34**, 65 (**1999**)

7. Barrie L.A., Bottenheim J.W., Schnell R.C., Crutzen P.J. and Rasmussen R.A., Ozone destruction and photochemical reactions at polar sunrise in the lower Arctic atmosphere, *Nature,* **334**, 138 **(1994)**

8. Bejanian Y., Bras G.L. and Poulet G., Kinetics and mechanism of IO+ClO reaction, *J. Phys. Chem.*, A**101,** 4088 (**1997**)

9. Bejanian Y., Bras G.L. and Poulet G., Photodissociation of the BrO radical, *J. Phys. Chem*., A**102,** 10501 (**1998**)

10. Gilles M.K., Turnipseed A.A., Burkholder J.B., Ravishankara A.R. and .Solomon S.J., Kinetics of the IO radical: 2. Reaction of IO with BrO, *J. Phys. Chem.*, A**101,** 5326 (**1997**)

11. Turnipseed A.A., Gilles M.K., Burkholder J.B. and Ravishankara A.R., Kinetics of the IO radical: 2. Reaction of IO with ClO, *J. Phys. Chem*., A**101,** 5517 (**1997**)

12. Turnipseed A.A., Birks J.W. and Calver J.G., Kinetics of the bromine monoxide radical + bromine monoxide radical reaction, *J. Phys. Chem*., **94**, 7477 **(1990)**

13. Rowley D. R., Bloss, W.J., Cox, R.A. and Jones R. L., Characterization of iodine species in the marine…, *J. Phys. Chem*., A**105,** 7855 (**2001**)

14. Johnsson K., Engdahl A., Koelm J, Nieminen J. and Nelander B., The ClOClO, BrOClO, and IOClO Molecules and Their Photoisomerization. A Matrix Isolation Study, *J. Phys. Chem*., **99**, 3902 (**1995**)

15. Guha S. and Francisco J.S., A density functional study of the structure, vibrational spectroscopy … $XBrO_2$ isomers (X=H,Cl,Br), *J. Phys. Chem*., A**101,** 5347 (**1997**), Grant D.J., Garner III E.B., Matus M.H., Nguyen M.T., Peterson K.A., Francisco J.S. and Dixon D.A., Thermochemical properties of XO_2, X_2O, XYO, X_2O_2 and XYO_2 (X,Y=Cl,Br,I) isomers, J. Phys. Chem. A**114,** 4254 (**2010**)

16. Melissas V.S., Papayannis D.K. and Kosmas A.M., Structural stability studies of IOOX peroxides (X=Cl, Br, I) and their isomers, *J. Mol. Struct.* (Theochem), **626**, 263 (**2003**)

17. Gomez P.C. and Pacios L.F., Bromine and mixed bromine chloride oxides: wave function… DFT calculation, J. Phys. Chem., A**103,** 739 (**1999**), Pacios L.F. and Gomez P.C, Ab initio study of bromine oxides OBrO and BrOO, *J. Phys. Chem*., A**101,** 1767 (**1997**)

18. Papayannis, D., Kosmas, A. M., Melissas, V. S., Quantum mechanical studies on the BrO self-reaction, *Chem. Phys*. **243**, 249 (**1999**)

19. Papayannis D.K., Kosmas A.M. and Melissas V.S., Quantum mechanical studies on the BrO+ClO reaction, *J. Phys. Chem.* A**105,** 2209 (**2001**)

20. Ghosh T.K. and Yabushita S., Ab initio study of the reaction kinetics of IO+ClO and IO+BrO, *Int. J. Res. Chem. Environ.*, **7**,7 (**2017**)

21. Ghosh T.K. and Yabushita S., Ab initio study of the isomers IOOCl reaction kinetics of IO+ClO, *Int. J. Res. Chem. Environ.*, **8**,1 (**2018**)

22. Martin J.M.L. and Sundermann A.J., Correlation consistent valence basis sets for…. core potential, *J. Chem. Phys*., **114,** 3408 (**2001**)

23. Basis sets and diffused functions are taken from http://www.emsl.pnl.gov:2080/forms/ basisform.html

24. Moore C.E., Atomic Energy Levels, NSRDS-NBS 35, Washington, DC, Vol. 1 and 3 (**1971**)

25. Chase Jr. M.W., NIST-JANAF Thermochemical Tables , *J. Phys. Chem. Ref. Data*, Monograph No. **9**, 4th ed. (**1998**)

26. Huber K.P. and Herzberg G., Molecular spectra and molecular structure: Constants of diatomic molecules, van Nostrand Reinhold, New York, Vol. IV, (**1979**)

27. Frisch M.J., et al., Gaussian 03W, Gaussian, Inc., Wallington, CT (**2005**)